Robotica (1998) volume 16, pp. 565–573. Printed in the United Kingdom © 1998 Cambridge University Press

Resolved-acceleration control of robot manipulators: A critical review with experiments

Fabrizio Caccavale, Ciro Natale, Bruno Siciliano and Luigi Villani

PRISMA Lab., Dipartimento di Informatica e Sistemistica, Università degli Studi di Napoli Federico II, Via Claudio 21, 80125 Napoli (Italy) {caccavale, natale, siciliano, villani}@disna.dis.unina.it

(Received in Final Form: November 26, 1997)

SUMMARY

The goal of this paper is to provide a critical review of the well-known resolved-acceleration technique for the tracking control problem of robot manipulators in the task space. Various control schemes are surveyed and classified according to the type of end-effector orientation error; namely, those based on Euler angles feedback, quaternion feedback, and angle/axis feedback. In addition to the assessed schemes in the literature, an alternative Euler angles feedback scheme is proposed which shows an advantage in terms of avoidance of representation singularities. An insight into the features of each scheme is given, with special concern to the stability properties of those schemes leading to nonlinear closed-loop dynamic equations. A comparison is carried out in terms of computational burden. Experiments on an industrial robot with open control architecture have been carried out, and the tracking performance of the resolved-acceleration control schemes in a case study involving the occurrence of a representation singularity is evaluated. The pros and cons of each scheme are evidenced in a final discussion focused on practical implementation issues.

KEYWORDS: Resolved-acceleration control; Euler angles feedback; Quaternion feedback; Angle/axis feedback; Industrial robot; Control schemes.

I INTRODUCTION

Robot tasks are naturally specified in terms of a sequence of manipulator configurations expressing the end-effector pose (position and orientation). Two main strategies can be adopted for motion control of a robot manipulator: joint space control and task space control. The former strategy requires the solution of an inverse kinematics problem to transform the desired end-effector motion into equivalent joint motions which constitute the reference inputs to a control scheme using joint position (and velocity) feedback. On the other hand, no inverse kinematics is required by the latter strategy and a feedback loop is closed directly on the end-effector pose (and velocity) variables. Even though joint space control is a congenial strategy used by industrial robots performing simple tasks, e.g. pick-and-place, task space control becomes essential to execute complex tasks, e.g. those requiring interaction between the end effector and the environment.[1]

In order to cope with the nonlinear and coupled nature of the manipulator dynamic model, inverse dynamics control can be pursued which consists of designing a model-based compensating action which globally linearizes and decouples the mechanical system in terms of a resolved task space acceleration;[2] this is chosen on the basis of the end-effector pose and velocity feedback so as to ensure stable tracking of the desired trajectory. The expression of the end-effector position error is rather obvious, whereas different definitions for the end-effector orientation error are feasible.

Since the direct kinematics equation of a robot manipulator is typically expressed in terms of an end-effector position vector and a rotation matrix, the original resolved-acceleration control scheme[2] used a feedback orientation error computed from the columns of the desired and the actual end-effector rotation matrix. As opposed to rotation matrix feedback, an error based on a minimal representation of orientation, e.g. Euler angles, was used in the operational space approach;[3] a drawback of this approach is the occurrence of representation singularities. An effective alternative to the above two descriptions is represented by a four-parameter singularity-free representation of the end-effector orientation error in terms of a unit quaternion, which has been successfully used for the attitude control problem of rigid bodies (spacecrafts)[4,5] and articulated bodies (manipulators).[6]

The contribution of this work is to present a critical review of resolved-acceleration control of robot manipulators with specific concern to the type of end-effector orientation error. In particular, three classes of schemes are surveyed; namely, those based on Euler angles feedback, quaternion feedback, and angle/axis feedback. In order to overcome the crucial drawback of representation singularities for the classical Euler angles feedback scheme, an alternative definition of orientation error based on Euler angles is proposed. The main features of each scheme are emphasized, and an insight into the stability analysis is provided for those schemes leading to nonlinear closed-loop dynamic equations.

The schemes are compared to one another on the basis of a computational burden analysis for the resolved angular acceleration.

Experimental tests on a setup comprising a 6-joint industrial robot Comau SMART-3S with open control architecture have been carried out. The tracking performance obtained with the various resolved-acceleration controllers is evaluated in a case study involving a motion in

https://doi.org/10.1017/S0263574798000290 Published online by Cambridge University Press

the neighbourhood of a representation singularity.

The paper ends with an extensive discussion focused on practical implementation issues related to computational complexity, tracking capability, trajectory planning, and the pros and cons of each scheme are highlighted.

II. BACKGROUND

The direct kinematics equation of an open kinematic chain robot manipulator is typically described in terms of the relationship between the $(n \times 1)$ vector $\boldsymbol{q}$ of joint variables and the (3×1) position vector $\boldsymbol{p}$ and the (3×3) rotation matrix

$$\boldsymbol{R} = [\boldsymbol{n}\ \ \boldsymbol{s}\ \ \boldsymbol{a}] \tag{1}$$

describing the origin and the orientation of the end-effector frame, where $\boldsymbol{n}$, $\boldsymbol{s}$, $\boldsymbol{a}$ are the unit vectors of the axes of the end-effector frame. The above quantities $\boldsymbol{p}$ and $\boldsymbol{R}$ are referred to a fixed base frame and no superscript is used; instead, if a matrix or vector quantity is to be referred to a frame other than the base frame, then a proper frame superscript shall be used.

The differential kinematics equation gives the relationship between the vector $\dot{\boldsymbol{q}}$ of joint velocities and the (6×1) vector $\boldsymbol{v} = [\dot{\boldsymbol{p}}^T\ \ \boldsymbol{\omega}^{\mathrm{T}}]^{\mathrm{T}}$ of the end-effector linear and angular velocities in the form

$$\boldsymbol{v} = \boldsymbol{J}(\boldsymbol{q})\dot{\boldsymbol{q}} \tag{2}$$

where $\boldsymbol{J}$ is the $(6 \times n)$ end-effector geometric Jacobian matrix; the joint configurtions at which the matrix $\boldsymbol{J}$ is not full-rank are termed kinematic singularities. The angular velocity is related to the time derivative of the rotation matrix by the notable relationship

$$\dot{\boldsymbol{R}} = \boldsymbol{S}(\boldsymbol{\omega})\boldsymbol{R} \tag{3}$$

where $\boldsymbol{S}$ is the skew-symmetric operator performing the cross product between two (3×1) vectors.

Equation (2) can be differentiated with respect to time to provide the relationship between the joint accelerations and the end-effector accelerations as

$$\dot{\boldsymbol{v}} = \boldsymbol{J}(\boldsymbol{q})\ddot{\boldsymbol{q}} + \dot{\boldsymbol{J}}(\boldsymbol{q}, \dot{\boldsymbol{q}})\dot{\boldsymbol{q}}. \tag{4}$$

The description based on the rotation matrix in (1) is inherently redundant, since $\boldsymbol{n}$*,* $\boldsymbol{s}$*,* $\boldsymbol{a}$ *are subject to six orthonormality constraints. A minimal representation of orientation can be obtained by using a set of three Euler angles* $\boldsymbol{\phi} = [\varphi\ \ \vartheta\ \ \psi]^{\mathrm{T}}$. Among the 12 possible definitions of Euler angles, the (Roll-Pitch-Yaw) *ZYX* representation can be considered leading to the rotation matrix

$$\boldsymbol{R}(\boldsymbol{\phi}) = \boldsymbol{R}_z(\varphi)\boldsymbol{R}_y(\vartheta)\boldsymbol{R}_x(\psi) \tag{5}$$

where $\boldsymbol{R}_z$, $\boldsymbol{R}_y$, $\boldsymbol{R}_x$ are the matrices of the elementary rotations about three independent coordinate axes of successive frames. The Euler angles can be extracted from a given rotation matrix by using closed-form inversion formulae.[1]

The relationship between the time derivative of the Euler angles $\dot{\boldsymbol{\phi}}$ and the end-effector angular velocity $\boldsymbol{\omega}$ is given by

$$\boldsymbol{\omega} = \boldsymbol{T}(\boldsymbol{\phi})\dot{\boldsymbol{\phi}} \tag{6}$$

where $\boldsymbol{T}$ is a transformation matrix that can be obtained from the time derivative of (5); this matrix is singular whenever $\vartheta = \pm\pi/2$ (representation singularity).

The further time derivative of (6) yields the acceleration relationship in the form

$$\dot{\boldsymbol{\omega}} = \boldsymbol{T}(\boldsymbol{\phi})\ddot{\boldsymbol{\phi}} + \dot{\boldsymbol{T}}(\boldsymbol{\phi}, \dot{\boldsymbol{\phi}})\dot{\boldsymbol{\phi}}. \tag{7}$$

An alternative description can be obtained by resorting to a four-parameter singularity-free representation in terms of a unit quaternion (viz. Euler parameters)

$$\eta = \cos\frac{\theta}{2} \tag{8}$$

$$\boldsymbol{\epsilon} = \sin\frac{\theta}{2}\boldsymbol{r}, \tag{9}$$

where θ and $\boldsymbol{r}$ are respectively the rotation and the (3×1) unit vector of an equivalent angle/axis description of orientation. Notice that the scalar part and the vector part of the quaternion are constrained by

$$\eta^2 + \boldsymbol{\epsilon}^{\mathrm{T}}\boldsymbol{\epsilon} = 1; \tag{10}$$

also $\{\eta, \boldsymbol{\epsilon}\}$ and $\{-\eta, -\boldsymbol{\epsilon}\}$ represent the same orientation. Hence, the end-effector frame is aligned with the base frame as long as $\eta = \pm 1$ and $\boldsymbol{\epsilon} = \boldsymbol{0}$. Several algorithms exist to extract the quaternion from a given rotation matrix; an efficient one is reported in reference 8, where the above sign ambiguity can be solved by choosing $\eta \geq 0$ for $\theta \in [-\pi, \pi]$ and taking into account the past values of the vector part to ensure continuity.

The relationship between the time derivative of the quaternion and the end-effector angular velocity is established by the so-called quaternion propagation:

$$\dot{\eta} = -\frac{1}{2}\boldsymbol{\epsilon}^{\mathrm{T}}\boldsymbol{\omega} \tag{11}$$

$$\dot{\boldsymbol{\epsilon}} = \frac{1}{2}\boldsymbol{E}(\eta, \boldsymbol{\epsilon})\boldsymbol{\omega} \tag{12}$$

with

$$\boldsymbol{E} = \eta\boldsymbol{I} - \boldsymbol{S}(\boldsymbol{\epsilon}). \tag{13}$$

The dynamic model of a robot manipulator can be written in the joint space as

$$\boldsymbol{B}(\boldsymbol{q})\ddot{\boldsymbol{q}} + \boldsymbol{C}(\boldsymbol{q}, \dot{\boldsymbol{q}})\dot{\boldsymbol{q}} + \boldsymbol{d}(\boldsymbol{q}, \dot{\boldsymbol{q}}) + \boldsymbol{g}(\boldsymbol{q}) = \boldsymbol{\tau}, \tag{14}$$

where $\boldsymbol{B}$ is the $(n \times n)$ symmetric positive definite inertia matrix, $\boldsymbol{C}\dot{\boldsymbol{q}}$ is the $(n \times 1)$ vector of Coriolis and centrifugal torques, $\boldsymbol{d}$ is the $(n \times 1)$ vector of friction torques, $\boldsymbol{g}$ is the $(n \times 1)$ vector of gravitational torques, and $\boldsymbol{\tau}$ is the $(n \times 1)$ vector of driving torques.

According to the well-known concept of inverse dynamics, the driving torques can be chosen as

$$\boldsymbol{\tau} = \boldsymbol{B}(\boldsymbol{q})\boldsymbol{J}^{-1}(\boldsymbol{q})(\boldsymbol{a} - \dot{\boldsymbol{J}}(\boldsymbol{q}, \dot{\boldsymbol{q}})\dot{\boldsymbol{q}}) + \boldsymbol{C}(\boldsymbol{q}, \dot{\boldsymbol{q}})\dot{\boldsymbol{q}} + \boldsymbol{d}(\boldsymbol{q}, \dot{\boldsymbol{q}}) + \boldsymbol{g}(\boldsymbol{q}), \tag{15}$$

where $\boldsymbol{a}$ is a new control input, and perfect dynamic compensation has been assumed; to this purpose, note that it is reasonable to assume compensation of the dynamic

https://doi.org/10.1017/S0263574798000290 Published online by Cambridge University Press

terms in the model (14), e.g. as obtained by a parameter identification technique.[7]

In deriving (15), a nonredundant manipulator ($n=6$) moving in a singularity-free region of the workspace has been considered to compute the inverse of the Jacobian. A damped least-squares inverse can be adopted to gain robustness in the neighbourhood of kinematic singularities,[9] whereas a pseudoinverse can be used in the redundant case ($n>6$) in conjunction with a suitable term in the null space of the Jacobian describing the internal motion of the manipulator.[10]

The vector $\boldsymbol{a}$ represents a resolved acceleration[2] which can be partitioned into its linear and angular components, i.e. $\boldsymbol{a}=[\boldsymbol{a}_p^{\mathrm{T}}\ \boldsymbol{a}_o^{\mathrm{T}}]^{\mathrm{T}}$. Substituting the control law (15) in (14) and accounting for (4) gives

$$\ddot{\boldsymbol{p}}_e=\boldsymbol{a}_p \tag{16}$$

$$\dot{\boldsymbol{\omega}}_e=\boldsymbol{a}_o \tag{17}$$

where subscript e refers to the actual end-effector pose. The goal is to design $\boldsymbol{a}_p$ and $\boldsymbol{a}_o$ so as to ensure tracking of the desired end-effector pose which is hereafter characterized by subscript d.

Let $\boldsymbol{p}_d$ and $\boldsymbol{p}_e$ respectively denote the desired and the actual end-effector position; the position error can be defined as

$$\Delta\boldsymbol{p}_{de}=\boldsymbol{p}_d-\boldsymbol{p}_e \tag{18}$$

where the operator Δ denotes that a vector difference has been taken, and the double subscript denotes that a mutual position is of concern. Then, the resolved linear acceleration can be chosen as

$$\boldsymbol{a}_p=\ddot{\boldsymbol{p}}_d+k_{Vp}\Delta\dot{\boldsymbol{p}}_{de}+k_{Pp}\Delta\boldsymbol{p}_{de} \tag{19}$$

where k_{Vp}, k_{Pp} are suitable feedback gains. Substituting (19) into (16) gives the closed-loop dynamic behaviour of the position error

$$\Delta\ddot{\boldsymbol{p}}_{de}+k_{Vp}\Delta\dot{\boldsymbol{p}}_{de}+k_{Pp}\Delta\boldsymbol{p}_{de}=\mathbf{0}. \tag{20}$$

The system (20) is exponentially stable for any choice of k_{Vp}, $k_{Pp}>0$, and thus tracking of $\boldsymbol{p}_d$ and $\dot{\boldsymbol{p}}_d$ is ensured.

As regards the resolved angular acceleration, $\boldsymbol{a}_o$ can be chosen in different ways, depending on the definition of end-effector orientation error used. Therefore, in the following three sections, various definitions of orientation error are considered which are classified into Euler angles feedback, quaternion feedback, and angle/axis feedback.

III. EULER ANGLES FEEDBACK

According to the classical operational space approach,[3] the most natural way of defining an orientation error is to consider an expression analogous to (18), i.e.

$$\Delta\boldsymbol{\phi}_{de}=\boldsymbol{\phi}_d-\boldsymbol{\phi}_e \tag{21}$$

where $\boldsymbol{\phi}_d$ and $\boldsymbol{\phi}_e$ are the set of Euler angles that can be extracted respectively from the rotation matrices $\boldsymbol{R}_d$ and $\boldsymbol{R}_e$ describing the orientation of the desired and the actual end-effector frame.

In view of (7), the resolved angular acceleration can be chosen as

$$\boldsymbol{a}_o=\boldsymbol{T}(\boldsymbol{\phi}_e)(\ddot{\boldsymbol{\phi}}_d+k_{Vo}\Delta\dot{\boldsymbol{\phi}}_{de}+k_{Po}\Delta\boldsymbol{\phi}_{de})+\dot{\boldsymbol{T}}(\boldsymbol{\phi}_e,\dot{\boldsymbol{\phi}}_e)\dot{\boldsymbol{\phi}}_e \tag{22}$$

where k_{Vo}, k_{Po} are suitable feedback gains. Substituting (22) into (17) gives the closed-loop dynamic behaviour of the orientation error

$$\Delta\ddot{\boldsymbol{\phi}}_{de}+k_{Vo}\Delta\dot{\boldsymbol{\phi}}_{de}+k_{Po}\Delta\boldsymbol{\phi}_{de}=\mathbf{0}. \tag{23}$$

where the matrix $\boldsymbol{T}(\boldsymbol{\phi}_e)$ shall be nonsingular. The system (23) is exponentially stable for any choice of k_{Vo}, $k_{Po}>0$; tracking of $\boldsymbol{\phi}_d$ and $\dot{\boldsymbol{\phi}}_d$ is ensured, which in turn implies tracking of $\boldsymbol{R}_d$ and $\boldsymbol{\omega}_d$.

The above Euler angles feedback becomes ill-conditioned when the actual end-effector orientation $\boldsymbol{\phi}_e$ becomes close to a representation singularity. In order to overcome this drawback, an alternative Euler angles feedback is proposed here which is based on the rotation matrix describing the mutual orientation between the desired and the actual end-effector frame, i.e.

$$\boldsymbol{R}_d^e=\boldsymbol{R}_e^{\mathrm{T}}\boldsymbol{R}_d. \tag{24}$$

Differentiating (24) with respect to time gives

$$\begin{aligned}\dot{\boldsymbol{R}}_d^e&=\boldsymbol{R}_e^{\mathrm{T}}(\boldsymbol{S}^{\mathrm{T}}(\boldsymbol{\omega}_e)+\boldsymbol{S}(\boldsymbol{\omega}_d))\boldsymbol{R}_d\\&=\boldsymbol{R}_e^{\mathrm{T}}\boldsymbol{S}(\boldsymbol{\omega}_d-\boldsymbol{\omega}_e)\boldsymbol{R}_e\boldsymbol{R}_e^{\mathrm{T}}\boldsymbol{R}_d\\&=\boldsymbol{S}(\Delta\boldsymbol{\omega}_{de}^e)\boldsymbol{R}_d^e\end{aligned} \tag{25}$$

where

$$\Delta\boldsymbol{\omega}_{de}=\boldsymbol{\omega}_d-\boldsymbol{\omega}_e \tag{26}$$

is the end-effector angular velocity error, and the properties of the skew-symmetric operator $\boldsymbol{S}$ in (3) have been exploited.

Let $\boldsymbol{\phi}_{de}$ denote the set of Euler angles that can be extracted from $\boldsymbol{R}_d^e$. Then, in view of (6) and (3), the angular velocity $\Delta\boldsymbol{\omega}_{de}^e$ in (25) is related to the time derivative of $\boldsymbol{\phi}_{de}$ as

$$\Delta\boldsymbol{\omega}_{de}^e=\boldsymbol{T}(\boldsymbol{\phi}_{de})\dot{\boldsymbol{\phi}}_{de}. \tag{27}$$

By taking the time derivative of (27), the resolved angular acceleration can be chosen as

$$\boldsymbol{a}_o=\dot{\boldsymbol{\omega}}_d-\dot{\boldsymbol{T}}_e(\boldsymbol{\phi}_{de})\dot{\boldsymbol{\phi}}_{de}+\boldsymbol{T}_e(\boldsymbol{\phi}_{de})(k_{Vo}\dot{\boldsymbol{\phi}}_{de}+k_{Po}\boldsymbol{\phi}_{de}) \tag{28}$$

where k_{Vo}, k_{Po} are suitable feedback gains and

$$\boldsymbol{T}_e(\boldsymbol{\phi}_{de})=\boldsymbol{R}_e\boldsymbol{T}(\boldsymbol{\phi}_{de}). \tag{29}$$

Substituting (28) into (17) gives the closed-loop dynamic behaviour of the orientation error

$$\ddot{\boldsymbol{\phi}}_{de}+k_{Vo}\dot{\boldsymbol{\phi}}_{de}+k_{Po}\boldsymbol{\phi}_{de}=\mathbf{0} \tag{30}$$

where the matrix $\boldsymbol{T}_e(\boldsymbol{\phi}_{de})$ shall be nonsingular. The system (30) is exponentially stable for any choice of k_{Vo}, $k_{Po}>0$; convergence to $\boldsymbol{\phi}_{de}=\mathbf{0}$ and $\dot{\boldsymbol{\phi}}_{de}=\mathbf{0}$ is ensured, which in turn implies tracking of $\boldsymbol{R}_d$ and $\boldsymbol{\omega}_d$.

The clear advantage of the alternative over the classical Euler angles feedback based on (21) is that, by adopting a representation $\boldsymbol{\phi}_{de}$ for which $\boldsymbol{T}(\mathbf{0})$ is nonsingular, representation singularities occur only for large orientation errors, e.g. when $\vartheta_{de}=\pm\pi/2$ for the *ZYX* representation. Notice that it is not advisable to choose the widely-adopted *ZYZ* represent-tion which is singular right at $\boldsymbol{\phi}_{de}=\mathbf{0}$! In other words, the

https://doi.org/10.1017/S0263574798000290 Published online by Cambridge University Press

ill-conditioning of matrix $\boldsymbol{T}$ is not influenced by the desired or actual end-effector orientation but only by the orientation error; hence, as long as the error parameter $|\vartheta_{de}|<\pi/2$, the behaviour of system (30) is not affected by representation singularities.

IV. QUATERNION FEEDBACK

In order to overcome the problem of representation singularities, the orientation error can be defined in terms of the vector part of the unit quaternion $\boldsymbol{\epsilon}^e_{de}$ that can be extracted from the rotation matrix $\boldsymbol{R}^e_d$ in (24).[6] The relationship with the angular velocity error in (26) is derived by applying the propagation rule (11), (12), i.e.

$$\dot{\eta}_{de}=-\frac{1}{2}\boldsymbol{\epsilon}^{e\mathrm{T}}_{de}\Delta\boldsymbol{\omega}^e_{de} \tag{31}$$

$$\dot{\boldsymbol{\epsilon}}^e_{de}=\frac{1}{2}\boldsymbol{E}(\eta_{de},\boldsymbol{\epsilon}^e_{de})\Delta\boldsymbol{\omega}^e_{de} \tag{32}$$

with $\boldsymbol{E}$ defined as in (13).

The resolved angular acceleration can be chosen as

$$\boldsymbol{a}_0=\dot{\boldsymbol{\omega}}_d+k_{Vo}\Delta\boldsymbol{\omega}_{de}+k_{Po}\boldsymbol{\epsilon}_{de} \tag{33}$$

where k_{Vo}, k_{Po} are suitable feedback gains and the orientation error has been referred to the base frame, i.e.

$$\boldsymbol{\epsilon}_{de}=\boldsymbol{R}_e\boldsymbol{\epsilon}^e_{de}. \tag{34}$$

Substituting (33) into (17) gives the closed-loop dynamic behaviour of the orientation error

$$\Delta\dot{\boldsymbol{\omega}}_{de}+k_{Vo}\Delta\boldsymbol{\omega}_{de}+k_{Po}\boldsymbol{\epsilon}_{de}=\boldsymbol{0}. \tag{35}$$

Differently from all the previous cases (20), (23), (30), the error system is nonlinear, and thus a Lyapunov argument is invoked to ascertain its stability.[4] Let

$$\begin{aligned} V&=k_{Po}((\eta_{de}-1)^2+\boldsymbol{\epsilon}^{\mathrm{T}}_{de}\boldsymbol{\epsilon}_{de})+\frac{1}{2}\Delta\boldsymbol{\omega}^{\mathrm{T}}_{de}\Delta\boldsymbol{\omega}_{de} \\ &=k_{Po}((\eta_{de}-1)^2+\boldsymbol{\epsilon}^{e\mathrm{T}}_{de}\boldsymbol{\epsilon}^e_{de})+\frac{1}{2}\Delta\boldsymbol{\omega}^{\mathrm{T}}_{de}\Delta\boldsymbol{\omega}_{de} \end{aligned} \tag{36}$$

be a positive definite Lyapunov function candidate. The time derivative of (36) along the trajectories of system (35) is

$$\begin{aligned} \dot{V}&=2k_{Po}((\eta_{de}-1)\dot{\eta}_{de}+\boldsymbol{\epsilon}^{e\mathrm{T}}_{de}\dot{\boldsymbol{\epsilon}}^e_{de})+\Delta\boldsymbol{\omega}^{\mathrm{T}}_{de}\Delta\dot{\boldsymbol{\omega}}_{de} \\ &=k_{Po}(-(\eta_{de}-1)\boldsymbol{\epsilon}^{e\mathrm{T}}_{de}\Delta\boldsymbol{\omega}^e_{de}+\boldsymbol{\epsilon}^{e\mathrm{T}}_{de}\boldsymbol{E}(\eta_{de},\boldsymbol{\epsilon}^e_{de})\Delta\boldsymbol{\omega}^e_{de}) \\ &\quad -k_{Vo}\Delta\boldsymbol{\omega}^{\mathrm{T}}_{de}\Delta\boldsymbol{\omega}_{de}-k_{Po}\Delta\boldsymbol{\omega}^{e\mathrm{T}}_{de}\boldsymbol{\epsilon}^e_{de} \\ &=-k_{Vo}\Delta\boldsymbol{\omega}^{\mathrm{T}}_{de}\Delta\boldsymbol{\omega}_{de} \end{aligned} \tag{37}$$

where (31), (32) have been exploited.

Since $\dot{V}$ is only negative semi-definite, in view of LaSalle's theorem, the system asymptotically converges to the invariant set described by the two equilibria:

$$\mathcal{Q}_1=\{\eta_{de}=-1,\quad \boldsymbol{\epsilon}_{de}=\boldsymbol{0},\quad \Delta\boldsymbol{\omega}_{de}=\boldsymbol{0}\} \tag{38}$$

$$\mathcal{Q}_2=\{\eta_{de}=1,\quad \boldsymbol{\epsilon}_{de}=\boldsymbol{0},\quad \Delta\boldsymbol{\omega}_{de}=\boldsymbol{0}\}. \tag{39}$$

The equilibrium $\mathcal{Q}_1$ is unstable. To see this, consider (36) which, in view of (37), is a decreasing function. At the equilibrium in (38), it is

$$V_E=4k_{Po}. \tag{40}$$

Take a small perturbation $\eta_{de}=-1+\sigma$ around the equilibrium with $\sigma>0$; then, it is $\boldsymbol{\epsilon}^{\mathrm{T}}_{de}\boldsymbol{\epsilon}_{de}=2\sigma-\sigma^2$. The perturbed Lyapunov function is

$$V_\sigma=4k_{Po}-2\sigma k_{Po}<V_E \tag{41}$$

and thus, since (36) is decreasing, V will never return to V_E, implying that $\mathcal{Q}_1$ is unstable. Therefore, the system must asymptotically converge to $\mathcal{Q}_2$, which in turn implies that tracking of $\boldsymbol{R}_d$ and $\boldsymbol{\omega}_d$ is achieved.

As a final remark, the closed-loop system with quaternion feedback (35) is nonlinear. If desired, a linear dynamics can be obtained for the orientation error $\boldsymbol{\epsilon}_{de}$, at the expense of a much more involved choice of the resolved angular acceleration.[11]

V. ANGLE/AXIS FEEDBACK

In the original resolved acceleration control scheme,[2] the orientation error was defined in terms of rotation matrix feedback as

$$\boldsymbol{o}_{de}=\frac{1}{2}(\boldsymbol{S}(\boldsymbol{n}_e)\boldsymbol{n}_d+\boldsymbol{S}(\boldsymbol{s}_e)\boldsymbol{s}_d+\boldsymbol{S}(\boldsymbol{a}_e)\boldsymbol{a}_d) \tag{42}$$

with the restriction $\boldsymbol{n}^{\mathrm{T}}_e\boldsymbol{n}_d>0$, $\boldsymbol{s}^{\mathrm{T}}_e\boldsymbol{s}_d>0$, $\boldsymbol{a}^{\mathrm{T}}_e\boldsymbol{a}_d>0$.

An equivalent expression of $\boldsymbol{o}_{de}$ is

$$\boldsymbol{o}_{de}=\sin\theta_{de}\boldsymbol{r}_{de} \tag{43}$$

where θ_{de} and $\boldsymbol{r}_{de}$ are respectively the rotation and the unit vector of an equivalent angle/axis description of the mutual orientation that can be extracted from the matrix

$$\boldsymbol{R}_{de}=\boldsymbol{R}_d\boldsymbol{R}^{\mathrm{T}}_e \tag{44}$$

which is referred to the base frame. Note that the above restriction related to (42) is equivalent to $\theta_{de}\in(-\pi/2,\pi/2)$. If θ_{de} were extended to the interval $(-\pi,\pi)$, the computation of the error in (43) would still be feasible although it would lead to a decreasing error norm for an increasing absolute value of the angle in the interval $(\pi/2,\pi)$.

In view of (8), (9), the orientation error in (43) can be also expressed in terms of a unit quaternion, i.e.

$$\boldsymbol{o}_{de}=2\eta_{de}\boldsymbol{\epsilon}_{de} \tag{45}$$

where $\{\eta_{de},\boldsymbol{\epsilon}_{de}\}$ can be extracted from (44). It can be shown[12] that the vector part of this quaternion coincides with (34), which has indeed motivated the use of the same symbol.

The time derivative of the orientation error (42) can be related to the desired and the actual end-effector angular velocity as[13]

$$\dot{\boldsymbol{o}}_{de}=\boldsymbol{L}^{\mathrm{T}}\boldsymbol{\omega}_d-\boldsymbol{L}\boldsymbol{\omega}_e \tag{46}$$

where

$$\boldsymbol{L}=-\frac{1}{2}(\boldsymbol{S}(\boldsymbol{n}_d)\boldsymbol{S}(\boldsymbol{n}_e)+\boldsymbol{S}(\boldsymbol{s}_d)\boldsymbol{S}(\boldsymbol{s}_e)+\boldsymbol{S}(\boldsymbol{a}_d)\boldsymbol{S}(\boldsymbol{a}_e)). \tag{47}$$

https://doi.org/10.1017/S0263574798000290 Published online by Cambridge University Press

The second time derivative is

$$\ddot{\boldsymbol{o}}_{de} = \boldsymbol{L}^{\mathrm{T}}\dot{\boldsymbol{\omega}}_d + \dot{\boldsymbol{L}}^{\mathrm{T}}\boldsymbol{\omega}_d - \boldsymbol{L}\dot{\boldsymbol{\omega}}_e - \dot{\boldsymbol{L}}\boldsymbol{\omega}_e. \tag{48}$$

The resolved angular acceleration can be chosen as

$$\boldsymbol{a}_0 = \boldsymbol{L}^{-1}(\boldsymbol{L}^{\mathrm{T}}\dot{\boldsymbol{\omega}}_d + \dot{\boldsymbol{L}}^{\mathrm{T}}\boldsymbol{\omega}_d - \dot{\boldsymbol{L}}\boldsymbol{\omega}_e + k_{Vo}\dot{\boldsymbol{o}}_{de} + k_{Po}\boldsymbol{o}_{de}), \tag{49}$$

where k_{Vo}, k_{Po} are suitable feedback gains, and $\boldsymbol{L}$ is nonsingular as long as the above restriction holds. In this respect, if the angle θ_{de} is extended to the interval $(-\pi, \pi)$, then a singularity occurs at $\theta_{de} = \pm\pi/2$ for the matrix $\boldsymbol{L}$ which does not allow the computation of $\boldsymbol{a}_o$ as in (49).

Substituting (49) into (17) gives the closed-loop dynamic behaviour of the orientation error

$$\ddot{\boldsymbol{o}}_{de} + k_{Vo}\dot{\boldsymbol{o}}_{de} + k_{Po}\boldsymbol{o}_{de} = \boldsymbol{0}, \tag{50}$$

which is a linear and decoupled system analogous to the position error system (20) as well to the orientation error systems (23), (30). Exponential stability is guaranteed for any choice of $k_{Vo}, k_{Po} > 0$; convergence to $\boldsymbol{o}_{de} = \boldsymbol{0}$ and $\dot{\boldsymbol{o}}_{de} = \boldsymbol{0}$ is ensured, which in turn implies tracking of $\boldsymbol{R}_d$ and $\boldsymbol{\omega}_d$.

Equation (49) reveals that the price to pay to obtain a linear and decoupled system is a large computational burden and the possible occurrence of a singularity. On the other hand, in the original rotation matrix feedback scheme[2] the resolved angular acceleration was simply chosen as

$$\boldsymbol{a}_0 = \dot{\boldsymbol{\omega}}_d + k_{Vo}\Delta\boldsymbol{\omega}_{de} + k_{Po}\boldsymbol{o}_{de}. \tag{51}$$

In this case, the closed-loop dynamic behaviour of the orientation error becomes

$$\Delta\dot{\boldsymbol{\omega}}_{de} + k_{Vo}\Delta\boldsymbol{\omega}_{de} + k_{Po}\boldsymbol{o}_{de} = \boldsymbol{0}. \tag{52}$$

The convergence analysis in reference 2 is valid only for small orientation errors. A Lyapunov stability analysis has been given later in reference 6 based on the expression of the orientation error in (45). However, a nonlinear k_{Po} is required to prove stability; this issue was addressed in reference 4 in the context of the attitude control problem.

Similarly to the quaternion feedback case above, a Lyapunov argument is invoked below to ascertain stability of system (52). Let

$$V = 2k_{Po}\boldsymbol{\epsilon}_{de}^{\mathrm{T}}\boldsymbol{\epsilon}_{de} + \frac{1}{2}\Delta\boldsymbol{\omega}_{de}^{\mathrm{T}}\Delta\boldsymbol{\omega}_{de} \tag{53}$$

$$= 2k_{Po}\boldsymbol{\epsilon}_{de}^{e\mathrm{T}}\boldsymbol{\epsilon}_{de}^{e} + \frac{1}{2}\Delta\boldsymbol{\omega}_{de}^{\mathrm{T}}\Delta\boldsymbol{\omega}_{de}$$

be a positive definite Lyapunov function candidate. The time derivative of (53) along the trajectories of system (52) is

$$\begin{aligned}\dot{V} &= 4k_{Po}\boldsymbol{\epsilon}_{de}^{e\mathrm{T}}\dot{\boldsymbol{\epsilon}}_{de}^{e} + \Delta\boldsymbol{\omega}_{de}^{\mathrm{T}}\Delta\dot{\boldsymbol{\omega}}_{de} \\ &= 2k_{Po}\boldsymbol{\epsilon}_{de}^{e\mathrm{T}}\boldsymbol{E}(\eta_{de}, \boldsymbol{\epsilon}_{de}^{e})\Delta\boldsymbol{\omega}_{de}^{e} \\ &\quad - k_{Vo}\Delta\boldsymbol{\omega}_{de}^{\mathrm{T}}\Delta\boldsymbol{\omega}_{de} - 2k_{Po}\eta_{de}\Delta\boldsymbol{\omega}_{de}^{e\mathrm{T}}\boldsymbol{\epsilon}_{de}^{e} \\ &= -k_{Vo}\Delta\boldsymbol{\omega}_{de}^{\mathrm{T}}\Delta\boldsymbol{\omega}_{de}\end{aligned} \tag{54}$$

where (31), (32) have been exploited.

Since $\dot{V}$ is only negative semi-definite, in view of LaSalle's theorem, the system asymptotically converges to the invariant set described by the following equilibria:

$$\mathcal{P}_1 = \{\eta_{de} = -1, \quad \boldsymbol{\epsilon}_{de} = \boldsymbol{0}, \quad \Delta\boldsymbol{\omega}_{de} = \boldsymbol{0}\} \tag{55}$$

$$\mathcal{P}_2 = \{\eta_{de} = 1, \quad \boldsymbol{\epsilon}_{de} = \boldsymbol{0}, \quad \Delta\boldsymbol{\omega}_{de} = \boldsymbol{0}\} \tag{56}$$

$$\mathcal{P}_3 = \{\eta_{de} = 0, \quad \boldsymbol{\epsilon}_{de} : \|\boldsymbol{\epsilon}_{de}\| = 1, \quad \Delta\boldsymbol{\omega}_{de} = \boldsymbol{0}\}. \tag{57}$$

The equilibria in the set $\mathcal{P}_3$ are all unstable. To see this, consider (53) which, in view of (54), is a decreasing function. At any equilibrium in (57), it is

$$V_E = 2k_{Po}. \tag{58}$$

Take a small perturbation $\eta_{de} = \sigma$ around such equilibrium; then, it is $\boldsymbol{\epsilon}_{de}^{\mathrm{T}}\boldsymbol{\epsilon}_{de} = 1 - \sigma^2$. The perturbed Lyapunov function is

$$V_\sigma = 2k_{Po} - 2\sigma^2 k_{Po} < V_E \tag{59}$$

and thus, since (53) is decreasing, V will never return to V_E, implying that the equilibria in $\mathcal{P}_3$ are unstable. Therefore, the system asymptotically converges to either $\mathcal{P}_1$ or $\mathcal{P}_2$; since both quaternions for those equilibria represent the same orientation, it can be concluded that tracking of $\boldsymbol{R}_d$ and $\boldsymbol{\omega}_d$ is achieved. Nevertheless, it is worth emphasizing that the equilibrium $\mathcal{P}_1$ is of no interest for the angle/axis feedback scheme based on (51) since it corresponds to an angle θ_{de} which is outside the interval $(-\pi, \pi)$ considered above.

An alternative angle/axis feedback scheme can be devised on the basis of the following expression for the orientation error

$$\boldsymbol{o}'_{de} = \theta_{de}\boldsymbol{r}_{de}. \tag{60}$$

The stability of the resulting closed-loop scheme can be analyzed in a formally similar way to the above, as discussed, e.g. in reference 9.

VI. COMPUTATIONAL ISSUES

The features of the above resolved-acceleration control schemes can be further investigated from a computational viewpoint. Since the main differences reside in the way the orientation feedback is defined, the analysis can be focused on the issues regarding the computation of the resolved angular acceleration. In this respect, it is assumed that the robot manipulator is controlled in a real-time fashion, and thus the planning of the desired end-effector trajectory shall be updated on the basis of sensory information about the surrounding environment where the robot operates. Therefore, the two key elements in the analysis are the trajectory generation and the computation of the orientation error.

The most congenial way for the user to specify a desired orientation trajectory is the equivalent angle/axis method.[1] Given the initial and final rotation matrices describing the orientation of the end-effector frame, the rotation matrix of the mutual orientation between the two frames is computed; the equivalent angle and axis unit vector are extracted, and the orientation trajectory is interpolated from zero to the total angle while keeping the unit vector constant. This method provides the user with a meaningful interpretation of the end-effector orientation along the trajectory from a geometric viewpoint, and thus is superior to the computationally lighter Euler angles method for which the intermediate orientations of the end-effector frame cannot

https://doi.org/10.1017/S0263574798000290 Published online by Cambridge University Press

be predicted beforehand. On the other hand, assigning the equivalent angle and axis directly leads to specifying a desired trajectory in terms of a unit quaternion via (8), (9). Upon these premises, it is assumed that the desired end-effector orientation trajectory is generated in terms of the rotation matrix $\boldsymbol{R}_d$; then, the angular velocity $\boldsymbol{\omega}_d$ and acceleration $\dot{\boldsymbol{\omega}}_d$ are simply computed from the time derivatives of the interpolating polynomial for the angle.

Regarding the actual orientation of the end-effector frame, this is typically available from the direct kinematics equation in terms of the rotation matrix $\boldsymbol{R}_e$ which can be computed from the joint position measurements; further, the actual end-effector angular velocity $\boldsymbol{\omega}_e$ can be computed from the joint velocity measurements via (2).

The computational burden of the schemes presented in the previous sections is evaluated in terms of the number of floating-point operations and transcendental functions needed to compute the resolved angular acceleration $\boldsymbol{a}_o$ where the additional computations needed for desired trajectory generation by those schemes not using $\boldsymbol{R}_d$, $\boldsymbol{\omega}_d$ and $\dot{\boldsymbol{\omega}}_d$ are evidenced. In particular, the angle/axis feedback scheme based on (49) has been ruled out in view of its inherent computational complexity. The results are reported in Table I, where the computations have been optimized whenever possible, e.g. by avoiding multiplications by zero and carrying out partial factorizations.

It can be recognized that the extraction of Euler angles augments the overall load for both feedback schemes, compared to the quaternion and the angle/axis feedback scheme. The interesting feature of the alternative Euler angles feedback scheme is the absence of extra computations for trajectory generation, which instead penalizes the classical Euler angles feedback scheme due to the extraction of Euler angles from $\boldsymbol{R}_d$ and the computation of their time derivatives. The computational load for the quaternion feedback scheme is smaller than for the Euler angles feedback schemes, even though an additional effort is required to compute the desired trajectory in terms of a unit quaternion. Not surprisingly, the angle/axis feedback scheme is the most computationally efficient since it operates directly on the desired and actual rotation matrices, the desired and actual angular velocities, and the desired angular acceleration.

VII. EXPERIMENTS

The laboratory setup consists of an industrial robot Comau SMART-3S (Fig. 1). The robot manipulator has a six-revolute-joint anthropomorphic geometry with nonnull shoulder and elbow offsets and non-spherical wrist. The joints are actuated by brushless motors via gear trains; shaft absolute resolvers provide motor position measurements. The robot is controlled by an open version of the C3G 9000 control unit[14] which has a VME-based architecture with a bus-to-bus communication link to a PC Pentium 133. This is in charge of computing the control algorithm and passing the references to the current servos through the communication link at 1 ms sampling rate. Joint velocities are reconstructed through numerical differentiation of joint position readings.

Table I. Computational load of the angular part for the resolved-acceleration control schemes

Angular feedback scheme	Resolved acceleration		Trajectory generation	
	Flops	Funcs	Flops	Funcs
Classical Euler	68	8	52	8
Alternative Euler	136	8	0	0
Quaternion	60	1	21	1
Angle/axis	55	0	0	0

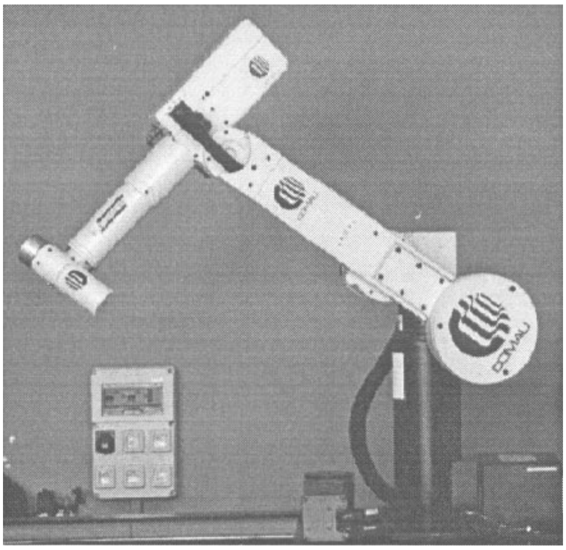

Fig. 1. Industrial robot Comau SMART-3S.

The dynamic model of the robot manipulator has been identified in terms of a minimum number of parameters, where the dynamics of the outer three joints has been simply chosen as purely inertial and decoupled. Only joint viscous friction has been included, since other types of friction (e.g. Coulomb and dry friction) are difficult to model.

The various resolved-acceleration control schemes have been implemented as C modules on the PC. The computational burden with the available hardware amounts to a total time of: 0.235 ms for the controller based on (15), (19), (22), 0.205 ms for the controller based on (15), (19), (28), 0.170 ms for the controller based on (15), (19), (33), and 0.155 ms for the controller based on (15), (19), (51). Notice that, with reference to the data in Table I, these times are inclusive also of the inverse dynamics computation, the basic trajectory generation and the manipulator kinematics computation, and of course the computation of the resolved linear acceleration.

The feedback gains of the above controllers have been set to: $k_{Vp}=75$ and $k_{Pp}=2500$ in (19), $k_{Vo}=75$ and $k_{Po}=2500$ in (22), (28), (51), while $k_{Vo}=75$ and $k_{Po}=5000$ in (33). These values have been chosen so as to assign the same dynamic behaviour to the various closed-loop error systems, where the nonlinear equations have been linearized for small orientation errors. In this way, a fair comparison can be carried out.

A case study has been developed to analyze the tracking performance of the various schemes. The end-effector desired position is required to make a straight line

https://doi.org/10.1017/S0263574798000290 Published online by Cambridge University Press

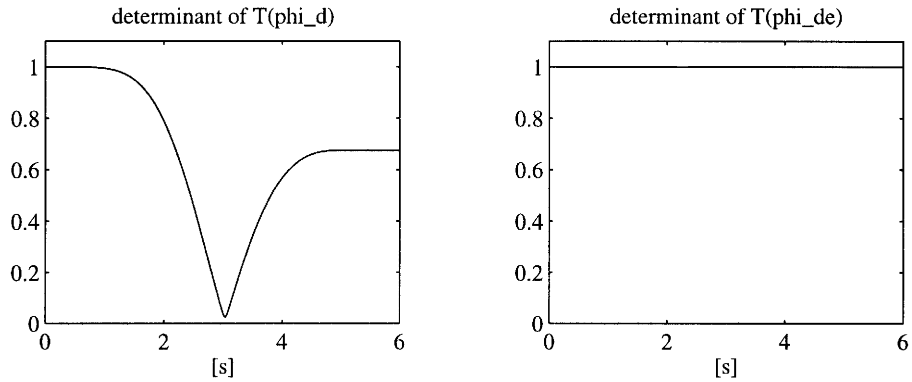

Fig. 2. Time histories of determinant of $\boldsymbol{T}(\boldsymbol{\phi}_d)$ and determinant of $\boldsymbol{T}(\boldsymbol{\phi}_{de})$.

displacement of (0.5, −0.6, 0.5) m along the coordinate axes of the base frame. The trajectory along the path is generated according to a 5-th order interpolating polynomial with null initial and final velocities and accelerations, and a duration of 5 s. The end-effector desired orientation is required to make a rotation of 3 rad about the axis (0.5639, 0.5840, −0.5840) with respect to the base frame. The trajectory is generated according to the equivalent angle/axis method, where the axis is fixed and the angle is interpolated by a 5-th order polynomial with null initial and final velocities and accelerations, and a duration of 5 s. The initial end-effector pose has been matched with the desired one.

As shown in the left-hand side of Figure 2, the desired

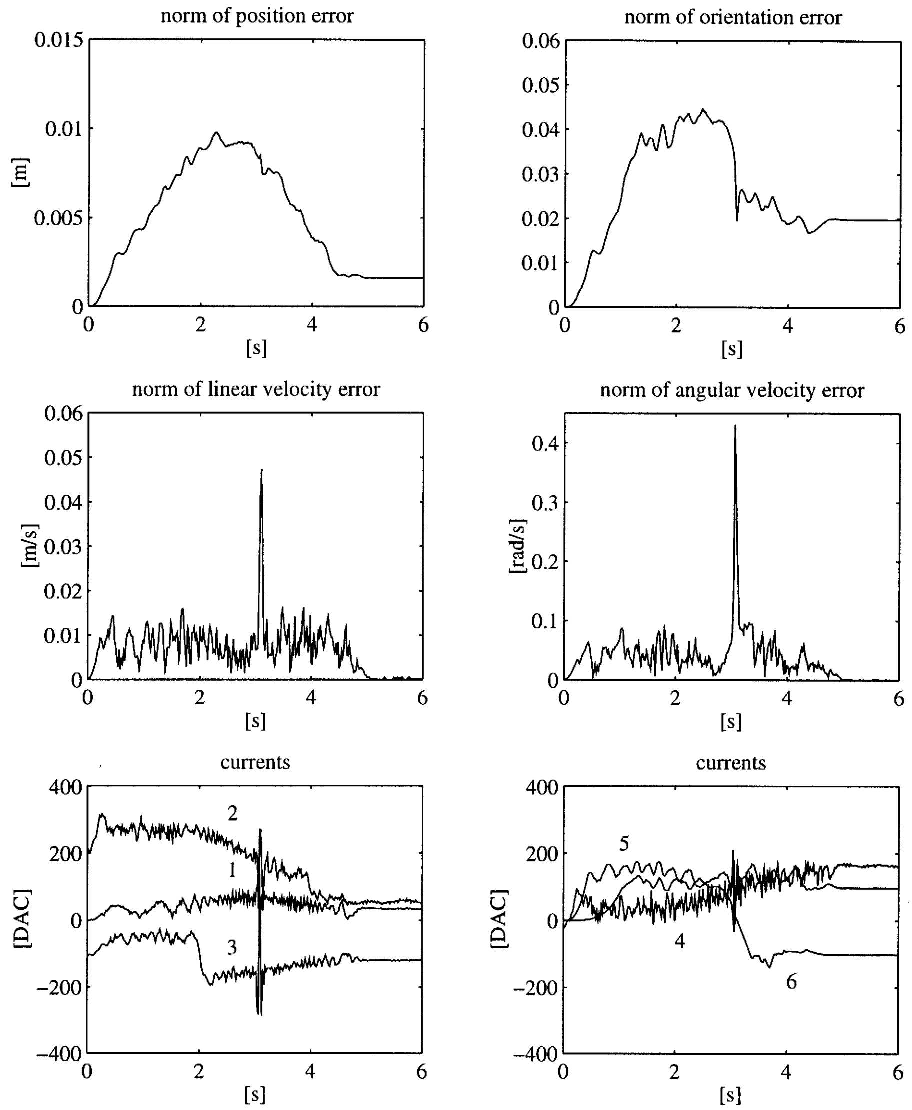

Fig. 3. Tracking performance of resolved-acceleration control based on (15), (19), (22).

https://doi.org/10.1017/S0263574798000290 Published online by Cambridge University Press

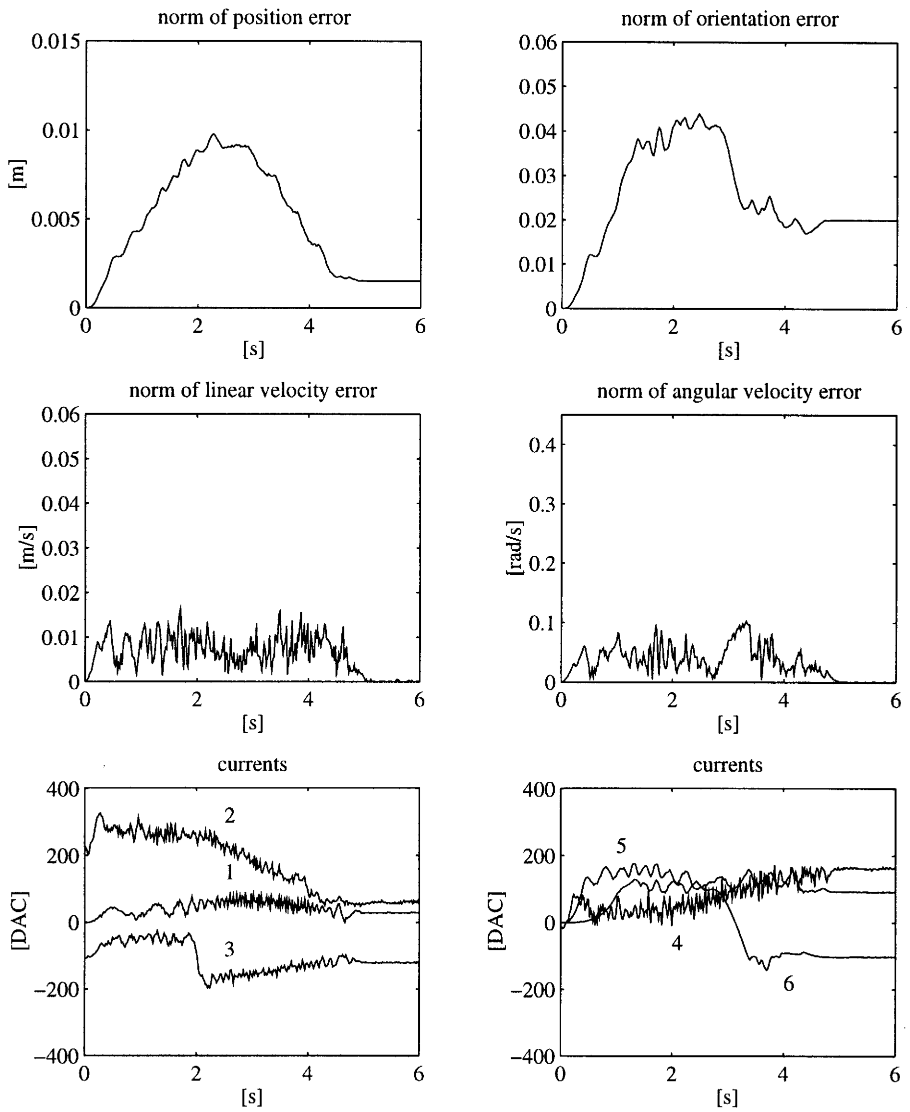

Fig. 4. Tracking performance of resolved-acceleration control based on (15), (19), (28).

end-effector orientation trajectory passes in the neighbourhood of a representation singularity for the matrix $\boldsymbol{T}(\boldsymbol{\phi}_d)$; this is a very demanding task in the face of the typical capability of a conventional industrial robot control unit.

The results are reported in Figs. 3 and 4 for the two Euler angles feedback schemes, the classical one and the alternative one proposed in this paper. The figures illustrate the time histories of the norm of the end-effector position error $\Delta\boldsymbol{p}_{de}$, the norm of an end-effector orientation error computed as the largest singular value of the matrix $(\boldsymbol{I}-\boldsymbol{R}_d^e)$, the norm of the linear velocity error $\Delta\dot{\boldsymbol{p}}_{de}$, the norm of the angular velocity error $\Delta\boldsymbol{\omega}_{de}$, and the joint reference motor currents (expressed in DAC units). Note that the choice of the above orientation error has been motivated by the desire of referring to a single measure of tracking performance for the various schemes, no matter what type of orientation feedback has been used.

It can be recognised that the performance in terms of the position and orientation errors is good for both schemes. The steady-state errors are nonnull because of the unavoidable imperfect compensation of static friction. A degradation of performance is observed in the linear and angular velocity errors for the scheme based on the classical Euler angles feedback; large peaks occur which are reflected also at the level of the motor currents. This phenomenon can be clearly understood because of the closeness to the representation singularity for the end-effector orientation in correspondence of the time instant when the determinant of $\boldsymbol{T}(\boldsymbol{\phi}_d)$ approaches zero. It should be remarked that its effect is visible not only on the angular velocity error but also on the linear velocity error, through the typical kinematic coupling between position and orientation in the non-spherical wrist manipulator. On the other hand, the scheme based on the alternative Euler angles feedback does not suffer from the occurrence of representation singularities, as confirmed in the right-hand side of Fig. 2 illustrating the determinant of the matrix $\boldsymbol{T}(\boldsymbol{\phi}_{de})$ which is nearly equal to one in view of the small orientation tracking error along the trajectory.

The overall tracking performance obtained with the quaternion feedback and the angle/axis feedback schemes is practically the same as that with the alternative Euler angles feedback scheme, and thus the numerical results have not been reported for brevity.

VIII. DISCUSSION

The previous sections have illustrated the analytical derivation, the stability analysis, the computational burden and the tracking performance for the various resolved-acceleration control schemes with special concern to the representation of the end-effector orientation error. In conclusion, a critical discussion is in order concerning the pros and cons of each scheme.

At first sight, the classical Euler angles feedback scheme might seem the simplest one in view of its similarity with the position feedback scheme. Nevertheless, the study has revealed that, besides the heavy computational load due to Euler angles extraction, there is no guarantee to avoid the occurrence of representation singularities even when good end-effector orientation tracking is achieved. On the other hand, the effort to plan a singularity-free orientation trajectory is considerable especially when the equivalent angle/axis method is adopted for meaningful task specification purposes.

The alternative Euler angles feedback scheme proposed in this paper has the main merit to almost overcome the above drawback of representation singularities, since it keenly operates on the set of Euler angles which is extracted from a single rotation matrix describing the mutual orientation between the desired and the actual end-effector frame. It may suffer only in the case of large orientation errors, but there is no practical worry for a convergent algorithm with matched initial conditions between the desired and the actual end-effector orientation. A weakness, however, is that the computational burden is still considerable.

The breakthrough of the quaternion feedback scheme stands in its applicability for any magnitude of the orientation error, since it is inherently based on a singularity-free representation of orientation. Its tracking performance is apparently as good as the alternative Euler angles feedback scheme, although the closed-loop orientation error dynamics is nonlinear. A further advantage is represented by the contained computational burden, even though the orientation error is not directly based on the desired and actual rotation matrices.

Finally, the angle/axis feedback scheme in the original resolved-acceleration control technique has the least computational load among all the schemes. Its performance is worse than that of the quaternion feedback scheme in the case of large orientation errors, whereas both schemes exhibit the same good behaviour for small orientation errors.

Acknowledgements

This work was supported in part by *MURST* and in part by *ASI.*

References

1. L. Sciavicco and B. Siciliano, *Modeling and Control of Robot Manipulators* (McGraw-Hill, New York, NY, 1996).
2. J.Y.S. Luh, M.W. Walker and R.P.C. Paul, ‘‘Resolved-acceleration control of mechanical manipulators’’ *IEEE Trans. on Automatic Control* **25,** 468–474 (1980).
3. O. Khatib, ‘‘A unified approach for motion and force control of robot manipulators: The operational space formulation’’ *IEEE J. of Robotics and Automation* **3,** 43–53 (1987).
4. J.T.-Y. Wen and K. Kreutz-Delgado, ‘‘The attitude control problem’ *IEEE Trans. on Automatic Control* **36,** 1148–1162 (1991).
5. O. Egeland and J.-M. Godhavn, ‘‘Passivity-based adaptive attitude control of a rigid spacecraft’’ *IEEE Trans. on Automatic Control* **39,** 842–846 (1994).
6. J.S.-C. Yuan, ‘‘Closed-loop manipulator control using quaternion feedback’’ *IEEE J. of Robotics and Automation* **4,** 434–440 (1988).
7. F. Caccavale and P. Chiacchio, ‘‘Identification of dynamic parameters and feedforward control for a conventional industrial manipulator’’ *Control Engineering Practice* **2,** 1039–1050 (1994).
8. S.W. Shepperd, ‘‘Quaternion from rotation matrix’’ *AIAA J. of Guidance and Control* **1,** 223–224 (1978).
9. C.W. Wampler and L.J. Leifer, ‘‘Applications of damped least-squares methods to resolved-rate and resolved-acceleration control of manipulators’’ *ASME J. of Dynamic Systems, Measurement, and Control* **110,** 31–38 (1988).
10. P. Hsu, J. Hauser and S. Sastry, ‘‘Dynamic control of redundant manipulators’ *J. of Robotic Systems* **6,** 133–148 (1989).
11. S.K. Lin, ‘‘Euler parameters in robot Cartesian control’’ *Proc. 1988 IEEE Int. Conf. on Robotics and Automation*, Philadelphia, PA (1988) pp. 1676–1681.
12. J.C.K. Chou, ‘‘Quaternion kinematic and dynamic differential equations’’ *IEEE Trans. on Robotics and Automation* **8,** 53–64 (1992).
13. S.K. Lin, ‘‘Singularity of a nonlinear feedback control scheme for robots’’ *IEEE Trans. on Systems, Man, and Cybernetics* **19**, 134–139 (1989).
14. F. Dogliani, G. Magnani and L. Sciavicco, ‘‘An open architecture industrial controller’’ *Newsl. of IEEE Robotics and Automation Soc.* **7,** No. 3, 19–21 (1993).